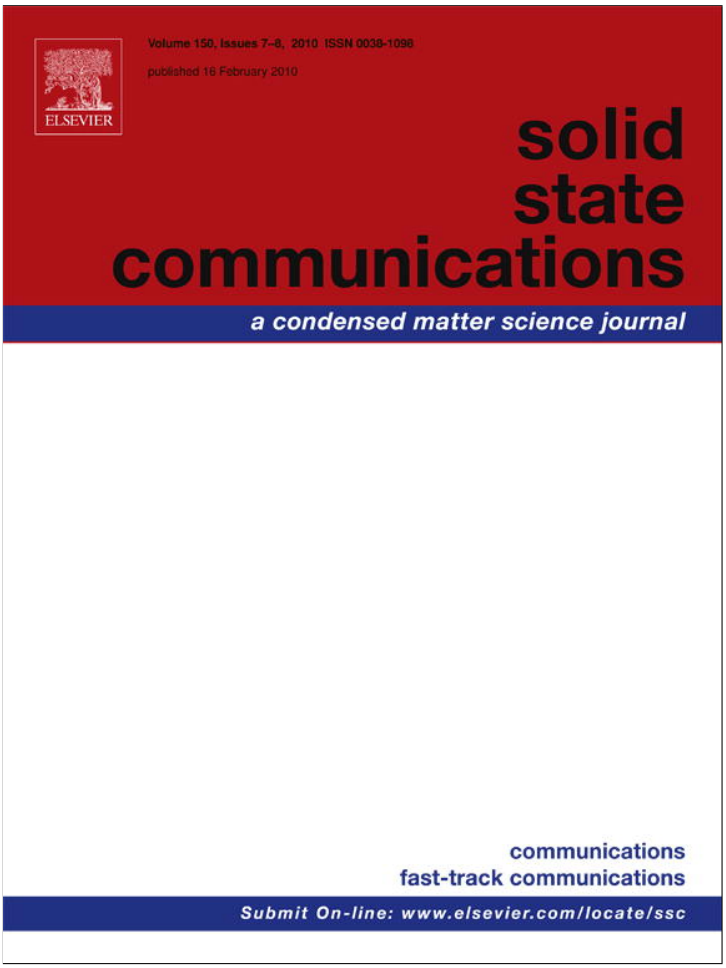

Solid State Communications 150 (2010) 341–345

Contents lists available at ScienceDirect

Solid State Communications

journal homepage: www.elsevier.com/locate/ssc

Complex magnetic phases in $LuFe_2O_4$

M.H. Phan [a], N.A. Frey [a,d], M. Angst [b,c], J. de Groot [b], B.C. Sales [c], D.G. Mandrus [c], H. Srikanth [a,*]

[a] Department of Physics, University of South Florida, Tampa, FL 33620, United States
[b] Institut für Festkörperforschung, JCNS, and JARA-FIT, Forschungszentrum Jülich GmbH, 52425 Jülich, Germany
[c] Materials Science and Technology Division, Oak Ridge National Laboratory, Oak Ridge, TN 37831, United States
[d] Department of Chemistry, Brown University, Providence, RI 02912, United States

ARTICLE INFO

Article history:
Received 9 August 2009
Received in revised form
11 November 2009
Accepted 18 November 2009
by J. Fontcuberta
Available online 26 November 2009

Keywords:
A. Magnetic oxide
D. Cluster glass
D. Magnetocaloric effect
E. Magnetic susceptibility

ABSTRACT

DC magnetization and AC susceptibility measurements on $LuFe_2O_4$ single crystals reveal a ferrimagnetic transition at 240 K followed by additional magnetic transitions at 225 K and 170 K, separating cluster glass phases, and a kinetically arrested state below 55 K. The origin of giant magnetic coercivity is attributed to the collective freezing of ferrimagnetic clusters and enhanced domain wall pinning associated with a structural transition at 170 K. Magnetocaloric effect measurements provide additional vital information about the multiple magnetic transitions and the glassy states. Our results lead to the emergence of a complex magnetic phase diagram in $LuFe_2O_4$.

1. Introduction

$LuFe_2O_4$ is a complex oxide of great current interest, as ferroelectricity in this material arises from charge ordering, and it also exhibits multiferroic behavior [1–3]. A clear understanding of the magnetic phase diagram has remained elusive, primarily due to the complexity of the system [4–9]. Notably, the giant magnetic coercivity (∼10 T at 4.2 K) and anomalous change in thermoremanent magnetization (TRM) were first reported 20 years ago [4,5], but their origin was not determined. In an attempt to explain the giant coercivity, Wu et al. [8] have recently argued that, in addition to undergoing a ferrimagnetic transition at $T_c \sim 240$ K, the $LuFe_2O_4$ system enters a glassy state at ∼80 K. They have attributed the coercivity enhancement below this temperature to the collective freezing of nanoscale pancake-like ferrimagnetic domains with large uniaxial magnetic anisotropy that were also imaged using magnetic force microscopy. While their discussion of glassy behavior and its impact on coercivity was restricted to the low-temperature (∼80 K) AC susceptibility peak that shows frequency dependence, their data (Fig. 1(a), (b) in [8]) also clearly displays frequency dependence at ∼225 K, indicative of glassy behavior, but this was not elaborated on. Meanwhile, recent studies by our group [9] and by Wang et al. [10] have confirmed that the $LuFe_2O_4$ system undergoes a glass transition at ∼225 K in addition to the ferrimagnetic transition at ∼240 K. We also observed an additional glass transition at ∼170 K, possibly similar to the glass transition feature at ∼80 K reported by Wu et al. [8]. These varied observations clearly indicate the complex magnetic nature of $LuFe_2O_4$ and thus demand further studies to understand the overall glass dynamics, magnetic phase diagram, onset of increase in coercivity just below ∼225 K [5,8] and the anomalous change in TRM [4,5] in this material.

In this communication, we present systematic DC magnetization, AC susceptibility, and magnetocaloric effect (MCE) measurements on $LuFe_2O_4$ single crystals. Our results indicate that $LuFe_2O_4$ undergoes a paramagnetic to ferrimagnetic transition at ∼240 K, followed by a re-entrant glass transition below ∼225 K and an additional first-order magnetic transition around 170 K, the last two of which both exhibit cluster glass characteristics [9]. The collective freezing of ferrimagnetic clusters below 225 K leads to the onset of increase in coercivity with further enhancement of the

* Corresponding address: Department of Physics, University of South Florida, PHY 114 4202 East Fowler Ave, Tampa, FL 33620, United States. Tel.: +1 813 974 2467; fax: +1 813 974 5813.
E-mail address: sharihar@cas.usf.edu (H. Srikanth).

0038-1098/$ – see front matter © 2009 Elsevier Ltd. All rights reserved.
doi:10.1016/j.ssc.2009.11.030

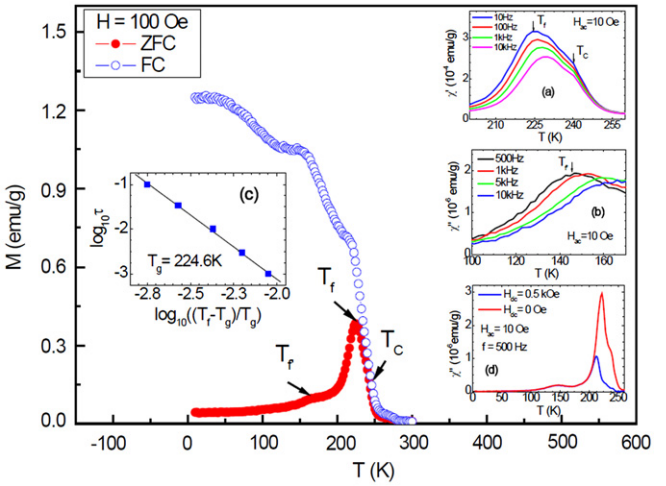

Fig. 1. Temperature dependence of field-cooled (FC) and zero-field-cooled (ZFC) magnetization. Insets (a) and (b) show the $\chi'(T)$ and $\chi''(T)$ curves for representative frequencies (f = 10 Hz–10 kHz) in the two temperature ranges around 225 K and 170 K, respectively. Inset (c) shows the best fit of $T_f(\omega)$ data extracted from AC susceptibility measurements [$\chi'(T)$] to the glass model Eq. (1) for the case of the peak at ∼225 K. Inset (d) shows the $\chi''(T)$ curves at a fixed frequency of 500 Hz for the cases H_{dc} = 0 and 0.5 kOe.

coercivity below 170 K attributed to enhanced domain wall pinning associated with the structural transition [11–13]. The formation of a kinetically arrested glassy state below 55 K is confirmed by MCE experiments. A comprehensive magnetic phase diagram is presented that also consistently accounts for many observations from other groups that were not fully understood.

2. Experimental

The $LuFe_2O_4$ single crystals were grown at ORNL by a floating zone technique, and details are described in [11]. The temperature dependences of the zero-field-cooled (ZFC) and field-cooled (FC) magnetization were measured on warming using a Physical Property Measurement System (PPMS) from Quantum Design in the temperature range 5–300 K at applied fields up to 70 kOe. The PPMS was also used for AC susceptibility measurements, performed upon warming up from 5 K. All the reported magnetic measurements were performed with the field along the c-axis of the $LuFe_2O_4$ crystal. For the purpose of comparison and consistency, the results featured in this paper are on crystals grown that show magnetization curves of qualitatively similar shapes to that commonly observed by other groups [4–8]. However, it should be noted that the neutron and X-ray scattering studies reported in [11–13] were on $LuFe_2O_4$ crystals that exhibited magnetization curves with sharper features at the characteristic transitions (240 K and 170 K). Sensitivity to sample growth conditions is well known in this system, although the presence of two magnetic transitions has now been confirmed by different groups, including us [4,10,11].

3. Results and discussion

Fig. 1 shows the ZFC and FC magnetization curves taken at 100 Oe applied field. The onset from the paramagnetic (PM) to the ferrimagnetic (FM) state occurs around 240 K, followed by a sharp peak in the ZFC curve at ∼225 K and a broader one around 170 K. Distinct changes in slopes at these temperatures are also observed in the FC curve. The two-peak feature was also reported by other groups [4,6,7], but the glassy nature of these peaks was not ascertained clearly. In the present study, the systematically collected AC susceptibility data show that the peaks at ∼225 K and ∼170 K are strongly frequency dependent (see insets (a) and (b) of Fig. 1). This indicates that $LuFe_2O_4$ undergoes glass transitions at these temperatures, in addition to the PM–FM transition at T_C ∼ 240 K, where $\chi'(T)$ rapidly decreases to zero and is frequency independent (see inset (a) of Fig. 1). While the $\chi'(T)$ (or $\chi''(T)$) peak at ∼225 K is quite sharp, the one at ∼170 K is somewhat broad, but the frequency dispersion is clearly visible from the $\chi''(T)$ data (see inset (b) of Fig. 1). For the $LuFe_2O_4$ single crystals studied by Wu et al. [8], the $\chi''(T)$ curve showed a sharp peak at ∼225 K and a broad peak at ∼80 K.

To quantitatively probe the glass dynamics in $LuFe_2O_4$, we have fitted the AC susceptibility data to a glass model expressed as [14]

$$\frac{\tau_{\max}}{\tau_0} = \left(\frac{T_f - T_g}{T_g}\right)^{-zv}, \quad (1)$$

where $\tau_{\max}$ is the maximum relaxation time, τ_0 is the microscopic flipping time of the fluctuating spins, T_f is the freezing temperature, T_g is the spin glass transition temperature, z is the dynamical exponent, and v is the usual critical exponent for the correlation length. The scaling of the AC susceptibility is plotted in inset (c) of Fig. 1 for the case of the peak at ∼225 K, and the best fit to Eq. (1) yields $T_g \approx 224.6$ K, $zv \approx 2.85$ and $\tau_0 \approx 9.18 \times 10^{-8}$ s. A similar procedure using the $\chi''(T)$ data for the case of the peak at ∼170 K yields $T_g \approx 137.5$ K, $zv \approx 3.12$ and $\tau_0 \approx 9.8 \times 10^{-6}$ s (note that instead of the $\chi'(T)$ data the $\chi''(T)$ data are used to fit the glass model because the peaks are much more visible and determined precisely, although the peak temperature ($T_{f'}$) for $\chi''(T)$ is lower than that (∼170 K) for $\chi'(T)$ or $M_{ZFC}(T)$). In both these cases, the obtained values of τ_0 are much larger than typical values for a conventional spin-glass system ($\tau_0 \sim 10^{-13}$ s) [13] but in good agreement with values found in cluster glass (CG) systems ($\tau_0 \sim 10^{-6}$–10^{-12} s) [15,16]. This quantitative analysis indicates that the magnetism in the $LuFe_2O_4$ system can be viewed as arising from an assembly of clusters. The difference in τ_0 for the two cases at ∼225 K ($\tau_0 \approx 9.18 \times 10^{-8}$ s) and ∼170 K ($\tau_0 \approx 9.8 \times 10^{-6}$ s) suggests a considerable difference in the size and distribution of clusters at these temperatures. Since a structural transition at ∼170 K has also been noted in the $LuFe_2O_4$ system [11–13], it can be argued that the structural transition directly affects the cluster size and distribution, leading to segregation of charge and thus creating an inhomogeneous magnetic structure (frustrated magnetism) at low temperatures. As T < 170 K, restructuring of ferrimagnetic clusters/domains would take place, resulting in enhanced wall number and increased pinning due to the new magnetic structure. Such a scenario has been reported in the literature for the case of doped manganites [17,18] and may be a general property of a larger class of correlated magnetic oxides. To verify this, we conducted AC susceptibility measurements at different applied DC magnetic fields and found that as the DC magnetic field (H_{dc}) was applied (below 2 T), the peak of $\chi''(T)$ at ∼225 K exhibited a significant shift to lower temperature, whereas the one at ∼170 K was largely unaffected relative to the case of H_{dc} = 0 (see, for example, inset (d) of Fig. 1). Based on these signatures, we attribute the feature at ∼170 K (seen in both $M_{ZFC}(T)$ and $\chi''(T)$ curves) to enhanced domain wall pinning due to the influence of a structural distortion at this temperature. This also explains the dynamic response of the spins decreasing (or the flipping time of the fluctuating spins increasing) for the case at ∼170 K ($\tau_0 \approx 9.8 \times 10^{-6}$ s) when compared with that at ∼225 K ($\tau_0 \approx 9.18 \times 10^{-8}$ s). Applying large DC magnetic fields (>2 T) leads to a complete suppression of the cluster glass transitions [19].

While the origin of the enhanced coercivity just below 225 K in $LuFe_2O_4$ was unclear in previous studies [5,8], our measurements and quantitative analysis of the AC susceptibility clearly indicate

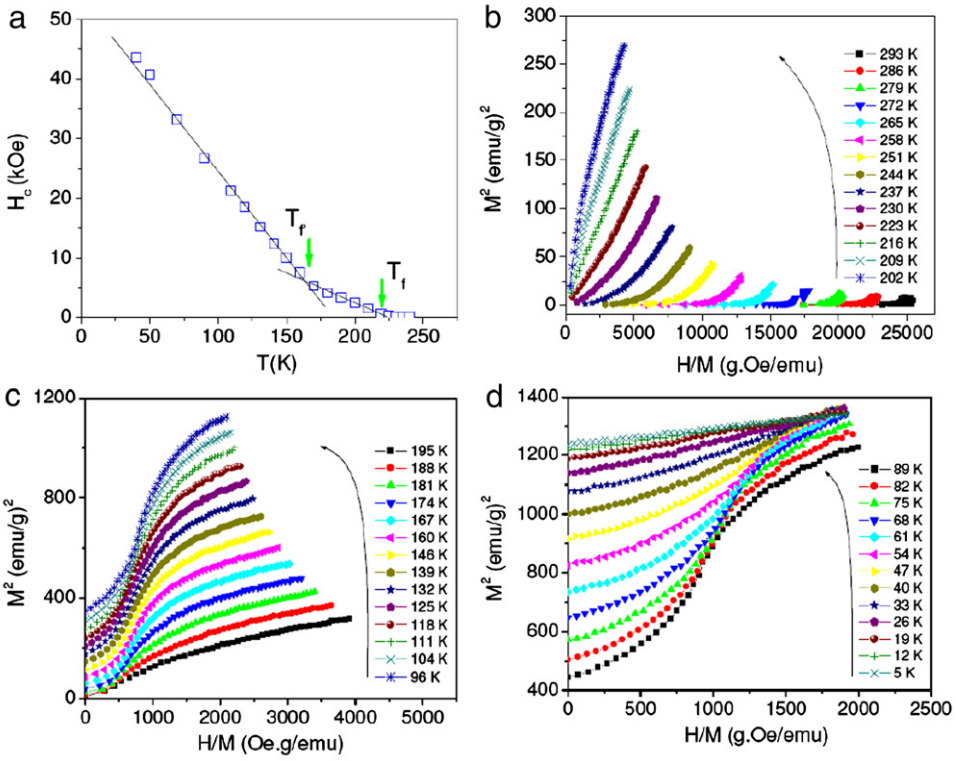

Fig. 2. (a) Temperature dependence of coercive field (H_c); (b)–(d) Arrott plots of magnetization curves for the three characteristic temperature ranges.

that $LuFe_2O_4$ undergoes a re-entrant cluster glass transition at ~225 K and the collective freezing of ferrimagnetic clusters results in large values of coercivity below this temperature (below T_f, see Fig. 2(a)). This observation is consistent with the fact that coercivity is often enhanced in the cluster glass state in amorphous alloys [20] below their freezing temperatures. As stated earlier, further enhancement of the coercivity below 170 K is attributed to enhanced domain wall pinning due to the occurrence of the structural transition (below $T_{f'}$; see Fig. 2(a)). The enhancement of coercivity due to the magnetic/structural transition has also been reported in $(CaSr)_2FeReO_6$ double perovskites [21]. Recently, Park et al. [22] have proposed through magnetic force microscopy (MFM) images and transmission electron microscopy (TEM) studies that enhanced pinning arises from the magnetoelectric coupling to charge-ordered superlattice domain boundaries, and this could probably lead to the enhanced coercivity at low temperatures in $LuFe_2O_4$ single crystals [8]. However, to clarify whether the enhanced pinning originates from the structural transition or the magnetoelectric coupling or both, further careful studies of the low-temperature structural transition and the coupling between charge order and magnetism in single crystals grown by various groups are needed.

To get a somewhat different perspective of the magnetic phase transitions in $LuFe_2O_4$, the measured data of the M–H isotherms were converted into H/M versus M^2 plots (the so-called Arrott plots) that are shown in Fig. 2(b)–(d). We recall that in an Arrott plot, where H/M is plotted against M^2, the curvature is expected to change at a specific temperature, where the magnetic ordering transition takes place. In the present case, there exist *three* characteristic temperature ranges over which the shapes of Arrott plots change sharply. Like the $H/M(T)$ plots, the Arrott plots indicate a ferrimagnetic transition at $T_c \sim 240$ K. However, they do not yield straight lines above and below T_c (see Fig. 2(b)), indicating that the $LuFe_2O_4$ system is not in a pure ferrimagnetic state with 3D magnetic ordering but rather this may be a signature of a quasi-2D magnetic order, which is not unreasonable given the layered structure of $LuFe_2O_4$. A notable change in the curvature is seen at temperatures below 225 K and 170 K, which are associated with the onset of the glassy behavior and its modification due to the structural transition, respectively. A further change in the curvature is seen in Fig. 2(d) for $T \leq 55$ K, with a note that, in this temperature range, the magnetization becomes almost unchanged as H_{dc} exceeds a critical value of 4.5 T. This is connected to the "kinetic arrest" picture of first-order transitions as found in doped $CeFe_2$ [23] and Gd_5Ge_4 [24] and recently also proposed for $LuFe_2O_4$ [13].

To gain further insights into the nature of magnetic ordering and arrested kinetics in $LuFe_2O_4$, we studied the magnetocaloric effect (i.e. the magnetic entropy change) in this material. While the MCE is generally considered in the community as an 'applied' measurement tool to probe magnetic refrigerant materials [25], it is actually a very useful probe of magnetic phase transitions, as we demonstrate clearly for this system. The magnetic entropy change $[\Delta S_M(T)]$ is calculated from a family of M–H isotherms using the Maxwell relation [25],

$$\Delta S_M(T, H_{\max}) = \mu_0 \int_0^{H_{\max}} \left(\frac{\partial M}{\partial T}\right)_H \mathrm{d}H, \tag{2}$$

where M is the magnetization, H is the magnetic field and T is the temperature. From Eq. (1), we note that $\Delta S_M(T)$ is directly related to the first derivative of magnetization with respect to temperature $(\partial M/\partial T)$ and so the MCE is expected to be inherently more sensitive for probing magnetic transitions than conventional magnetization and resistivity measurements. A very small change in M can give rise to a more pronounced effect in $\Delta S_M(T)$ than in $M(T)$ or $R(T)$. Importantly, the sign of ΔS_M, which is determined by the slope change of the $\mathrm{d}M/\mathrm{d}T$ curve, can allow probing the magnetic transitions further to better understand the nature of the different phases in a material with a rich and complex H–T magnetic phase diagram [26]. Following the convention in MCE analysis, the value of $-\Delta S_M$ is *positive* for materials exhibiting

an FM transition, because of the fully magnetically ordered configuration with the application of external magnetic field [25,27]. Meanwhile, *negative* values of $-\Delta S_M$ are found in AFM ordering systems due to orientational disorder of the magnetic sublattice anti-parallel to the applied magnetic field [28,29]. The temperature dependence of magnetic entropy change for $LuFe_2O_4$ is presented in Fig. 3. Clearly, the $\Delta S_M(T)$ curves show three peaks, which are associated with the glass transition temperatures (at ~225 K and ~170 K, respectively (as seen in the ZFC magnetization of Fig. 1) and the noted temperature (~55 K). The small discrepancy in the temperature peaks seen in the $\Delta S_M(T)$ curves from those seen in the M–T data can be attributed to the occurrence of multiple magnetic transitions. Franco et al. [30] have recently shown that the temperature peaks determined from the $\Delta S_M(T)$ data do not necessarily coincide with those determined from the M–T data, even for homogeneous systems. In the present study, it is worth noting that the *positive* values of $-\Delta S_M$ obtained for $LuFe_2O_4$ evidently exclude the dominance of AFM ordering in this material. This is consistent with our argument that the peak in ZFC magnetization at ~225 K is not due to a Néel-type antiferromagnetic transition but rather associated with the re-entrant cluster glass transition. Furthermore, the difference in magnitude between the maximum $-\Delta S_M$ at the transition temperatures (denoted as T_{p1}, T_{p2} and T_{p3} in Fig. 3) suggests different mechanisms for magnetic interactions in $LuFe_2O_4$ at temperatures below 240 K. It can be seen in inset (a) of Fig. 3 that the magnitude of the maximum $-\Delta S_M$ for the case of peaks T_{p1} and T_{p2} varies linearly with the applied magnetic field, whereas for the case of T_{p3} it first increases with increasing $\Delta\mu_0 H$ up to 4.5 T and then remains unchanged for $\Delta\mu_0 H > 4.5$ T. We attribute the linear change of the maximum $-\Delta S_M$ for T_{p1} and T_{p2} to the gradual orientation of ferrimagnetic domains/clusters with increasing applied magnetic field. The smaller value of the maximum $-\Delta S_M$ for T_{p2} compared to that for T_{p1} is the result of increased local disorder (enhanced wall pinning) due to the intervening structural transition at this temperature. By contrast, for the case of T_{p3} the constancy of both the maximum $-\Delta S_M$ (see inset (a) of Fig. 3) and its peak temperature (see inset (b) of Fig. 3) for $\Delta\mu_0 H > 4.5$ T is the result of a glass-like kinetic arrest of the first-order transition at $T < 55$ K, where the system becomes fully frozen as the applied magnetic field exceeds a critical value (~4.5 T). This arrested state is clearly formed with the assistance of an external magnetic field ($H > 4.5$ T—the critical magnetic field). This important observation allows one to explain the origin of the anomalous change of TRM at low temperatures observed by Iida et al. [4,5]; the TRM was temperature and magnetic field independent below ~60 K (which means that the system enters a kinetically arrested glassy state at ~60 K) and the hysteresis in TRM appeared to occur between ~60 K and ~140 K (which agrees well with the presence of a first-order magnetic transition).

Finally, a magnetic phase diagram which is established from the magnetic and magnetocaloric data is presented in Fig. 4. A paramagnetic–ferrimagnetic (PM–FM) transition at ~240 K is followed by a re-entrant cluster glass (CG) transition (namely, the CG1 state) at ~225 K, further by a second CG transition (namely, the CG2 state) below 170 K, and finally a kinetically arrested glassy state is entered below 55 K. In fact, the kinetics is partially arrested at temperatures between 55 K and 65 K (65 K is considered as the temperature at which the kinetic arrest starts to occur) and is completely arrested below 55 K. Similar behavior was also observed, for example, for Gd_5Ge_4 [24]. An important fact that emerges from this magnetic phase diagram is that the occurrence of a structural transition around 170 K affects the size and distribution of ferrimagnetic clusters in the CG1 state, thus creating a new configuration of ferrimagnetic clusters in the CG2 state and consequently altering the spin dynamics in $LuFe_2O_4$.

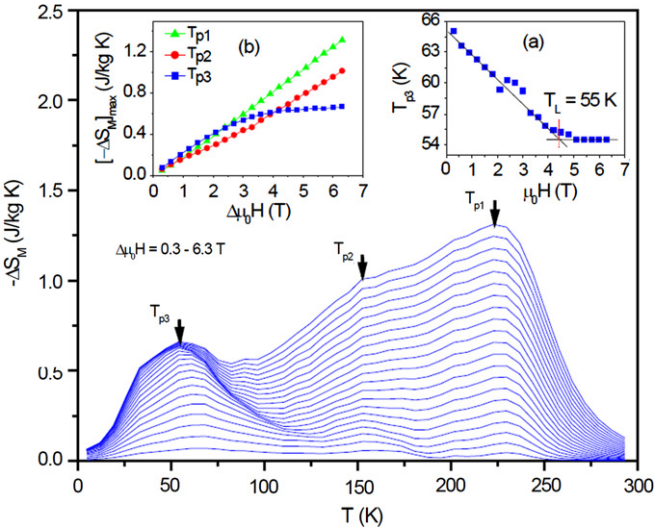

Fig. 3. Temperature dependence of the magnetic entropy change $-\Delta S_M(T)$ at different applied magnetic fields. Inset (a) shows the magnetic field dependence of the maximum magnetic entropy change ($-\Delta S_M^{Tp1}$, $-\Delta S_M^{Tp2}$ and $-\Delta S_M^{Tp3}$) corresponding to the peaks T_{p1}, T_{p2} and T_{p3}. Inset (b) shows the magnetic field dependence of the peak temperature at T_{p3}.

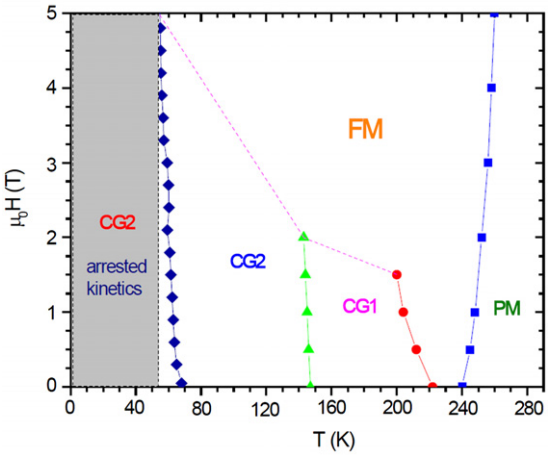

Fig. 4. Magnetic phase diagram. A paramagnetic to ferrimagnetic (PM–FM) transition at ~240 K is followed by a re-entrant cluster glass transition (CG1 state) at ~225 K and further by a second CG transition (CG2 state) below 170 K, partial kinetic arrest below 65 K and complete arrest below 55 K. Square symbols: data taken from the $M_{FC}(T)$ data measured at different DC magnetic fields; circle symbols: data from the $\chi'(T)$ data measured at different DC magnetic fields; triangle symbols: data from the $\chi''(T)$ data measured at different DC magnetic fields; tetragonal symbols: data from the MCE data (i.e. $T_{p3}(H)$ from inset (b) of Fig. 3).

Acknowledgements

The work at USF was supported by DOE BES Physical Behavior of Materials Program through grant number DE-FG02-07ER46438. The research at ORNL was sponsored by the Division of Materials Sciences and Engineering, Office of Basic Energy Sciences, US Department of Energy.

References

[1] N. Ikeda, H. Ohsumi, K. Ishii, T. Inami, K. Kakurai, Y. Murakami, K. Yoshii, S. Mori, Y. Horibe, H. Kito, Nature 436 (2005) 1136.
[2] M.A. Subramanian, T. He, J. Chen, N.S. Rogado, T.G. Calvarese, A.W. Sleight, Adv. Mater. 18 (2006) 1737.
[3] H.J. Xiang, M.-H. Whangbo, Phys. Rev. Lett. 98 (2007) 246403.
[4] J. Iida, Y. Nakagawa, N. Kimizuka, J. Phys. Soc. Japan 55 (1986) 1434.
[5] J. Iida, M. Tanaka, Y. Nakagawa, S. Funahashi, N. Kimizuka, S. Takekawa, J. Phys. Soc. Japan 62 (1993) 1723.

[6] K. Yoshii, N. Ikeda, Y. Matsuo, Y. Horibe, S. Mori, Phys. Rev. B 76 (2007) 024423.
[7] Y. Zhang, H.X. Yang, Y.Q. Guo, C. Ma, H.F. Tian, J.L. Luo, J.Q. Li, Phys. Rev. B 76 (2007) 184105.
[8] W. Wu, V. Kiryukhin, H.-J. Noh, K.-T. Ko, J.-H. Park, W. Ratcliff II, P.A. Sharma, N. Harrison, Y.J. Choi, Y. Horibe, S. Lee, S. Park, H.T. Yi, C.L. Zhang, S.-W. Cheong, Phys. Rev. Lett. 101 (2008) 137203.
[9] M.H. Phan, J. Gass, N.A. Frey, H. Srikanth, M. Angst, B.C. Sales, D. Mandrus, J. Appl. Phys. 105 (2009) 07E308.
[10] F. Wang, J. Kim, Y.J. Kim, Phys. Rev. B. 80 (2009) 024419.
[11] A.D. Christianson, M.D. Lumsden, M. Angst, Z. Yamani, W. Tian, R. Jin, E.A. Payzant, S.E. Nagler, B.C. Sales, D. Mandrus, Phys. Rev. Lett. 100 (2008) 107601.
[12] M. Angst, R.P. Hermann, A.D. Christianson, M.D. Lumsden, C. Lee, M.-H. Whangbo, J.-W. Kim, P.J. Ryan, S.E. Nagler, W. Tian, R. Jin, B.C. Sales, D. Mandrus, Phys. Rev. Lett. 101 (2008) 227601.
[13] X.S. Xu, M. Angst, T.V. Brinzari, R.P. Hermann, J.L. Musfeldt, A.D. Christianson, D. Mandrus, B.C. Sales, S. McGill, J.-W. Kim, Z. Islam, Phys. Rev. Lett. 101 (2008) 227602.
[14] A.P. Young (Ed.), Spin Glasses and Random Fields, in: Series on Directions in Condensed Matter Physics, vol. 12, World Scientific, Singapore, 1998.
[15] S. Mukherjee, R. Ranganathan, P.S. Anilkumar, P.A. Joy, Phys. Rev. B 54 (1996) 9267.
[16] D.N.H. Nam, K. Jonason, P. Nordblad, N.V. Khiem, N.X. Phuc, Phys. Rev. B 59 (1999) 4189.
[17] T. Shibata, B. Bunker, J.F. Mitchell, P. Schiffer, Phys. Rev. Lett. 88 (2002) 207205.
[18] K. Mukherjee, A. Banerjee, Phys. Rev. B 77 (2008) 024430.
[19] As the DC magnetic field increases, the $\chi(T)$ peaks at ∼225 K and ∼170 K decrease and finally disappear at $H_{dc} \sim 1.5$ T and ∼2 T, respectively.
[20] T. Miyazaki, I. Okamoto, Y. Ando, M. Takahashi, J. Phys. F 18 (1988) 1601.
[21] J.M. De Teresa, D. Serrate, J. Blasco, M.R. Ibarra, L. Morellon, Phys. Rev. B 69 (2004) 144401.
[22] S. Park, Y. Horibe, Y.J. Choi, C.L. Zhang, S.-W. Cheong, W. Wu, Phys. Rev. B 79 (2009) 180401.
[23] M.K. Chattopadhyay, S.B. Roy, P. Chaddah, Phys. Rev. B 72 (2005) 180401.
[24] J.D. Moore, G.K. Perkins, K. Morrison, L. Ghivelder, M.K. Chattopadhyay, S.B. Roy, P. Chaddah, K.A. Gschneidner, V.K. Pecharsky, L.F. Cohen, J. Phys.: Condens. Matter 20 (2008) 465212.
[25] M.H. Phan, S.C. Yu, J. Magn. Magn. Mater. 308 (2007) 325.
[26] A. Biswas, T. Samanta, S. Banerjee, I. Das, Appl. Phys. Lett. 92 (2008) 012502.
[27] M.H. Phan, G.T. Woods, A. Chaturvedi, S. Stefanoski, G.S. Nolas, H. Srikanth, Appl. Phys. Lett. 93 (2008) 252505.
[28] P. Sande, L.E. Hueso, D.R. Miguens, J. Rivas, F. Rivadulla, M.A. Lopez-Quintela, Appl. Phys. Lett. 79 (2001) 2040.
[29] M.S. Reis, V.S. Amaral, J.P. Araujo, P.B. Tavares, A.M. Gomes, I.S. Oliveira, Phys. Rev. B 71 (2005) 144413.
[30] V. Franco, A. Conde, M.D. Kuzmin, J.M. Romero-Enrique, J. Appl. Phys. 105 (2009) 07A917.